

RESEARCH

Open Access



Effect of time-restricted feeding and caloric restriction in metabolic associated fatty liver disease in male rats

Jiang Deng^{1†}, Juan Ma^{1†}, Xin Zhang², Kairuo Wang¹, Yikai Wang², Ning Gao², Dandan Feng², Xiaoli Jia², Xiongtao Liu³, Shuangsoo Dang^{2†} and Juanjuan Shi^{2*†}

Abstract

Background The prevalence of metabolic associated fatty liver disease (MAFLD) is high. However, there are few studies on the effects of time-restricted feeding (TRF) and caloric restriction (CR) in MAFLD.

Objectives To investigate the efficacy and mechanism of 4 h TRF and 60% CR in MAFLD.

Methods Twelve male Sprague–Dawley rats were randomly assigned to the Normal group (normal diet, 10 kcal% fat), while the remaining 38 rats were assigned to the MAFLD group (high-fat diet, 60 kcal% fat). 10 weeks later, the MAFLD group was randomly divided into the 4 h TRF, 60% CR, 4 h TRF + 60% CR, and Model groups; all rats were then given normal diet. After 4 weeks, weight, blood lipid, and other indicators were detected.

Results After the high-fat diet was discontinued, the liver lipid levels in the rat with MAFLD significantly reduced, while the body weight was not significantly changed. The rats in the Model group were heavier than those in the other four groups ($p < 0.01$). The triglyceride levels were higher in the TRF + CR group compared with the Model group ($p < 0.01$). Compared with the Model group, 110 metabolites were decreased in the TRF + CR group, and 83 metabolites were elevated in liver. Kyoto Encyclopedia of Genes and Genomes revealed that the mechanism involved the proliferator–activated receptor alpha signaling pathway, metabolic pathway, and so on. We observed differences in silent information regulator transcript 1 (*SIRT1*) mRNA levels in all five groups ($p = 0.003$).

Conclusions 4 h TRF and 60% CR significantly reduced body weight and liver lipid in rats with MAFLD. 4 h TRF can improve MAFLD, and there is no need to excessively restrict food intake.

Keywords Metabolic associated fatty liver disease, Intermittent fasting, Time restricted feeding, Caloric restriction, Triglycerides

[†]Jiang Deng, Juan Ma, Shuangsoo Dang, and Juanjuan Shi have equally contributed to this work.

*Correspondence:

Juanjuan Shi

juanjuan_shi@xjtu.edu.cn

Full list of author information is available at the end of the article



© The Author(s) 2025. **Open Access** This article is licensed under a Creative Commons Attribution-NonCommercial-NoDerivatives 4.0 International License, which permits any non-commercial use, sharing, distribution and reproduction in any medium or format, as long as you give appropriate credit to the original author(s) and the source, provide a link to the Creative Commons licence, and indicate if you modified the licensed material. You do not have permission under this licence to share adapted material derived from this article or parts of it. The images or other third party material in this article are included in the article's Creative Commons licence, unless indicated otherwise in a credit line to the material. If material is not included in the article's Creative Commons licence and your intended use is not permitted by statutory regulation or exceeds the permitted use, you will need to obtain permission directly from the copyright holder. To view a copy of this licence, visit <http://creativecommons.org/licenses/by-nc-nd/4.0/>.

Introduction

Living standards have greatly improved with increased global productivity, but excessive nutritional intake has become increasingly prevalent [1]. In the past 10 years in China, the prevalence of nonalcoholic fatty liver disease (NAFLD) has risen markedly, from 18 to 29.2% [2], while the global prevalence is 25.2% and often higher in some certain regions [3]. NAFLD is now known as metabolic associated fatty liver disease (MAFLD). Currently, there is a lack of specific treatments for MAFLD, and management largely focus on diet control and increased physical activity. Caloric restriction (CR) needs to calculate the calories contained in food, which presents challenges and limits its application in daily life. Counting calories is hard, but eating fewer calories can be even harder. In addition to CR, intermittent fasting (IF) is an ancient diet therapy that requires no or very little caloric intake for a certain period, typically lasting more than 12 h, to prevent disease by alternating between a normal eating state and a fasting state [4]. The IF protocols include alternate-day fasting, time-restricted feeding (TRF), and 5:2 fasting. Studies by others have reported that IF help prevent obesity, type 2 diabetes, and other metabolic diseases [5, 6]. Thus, IF may be a promising strategy for improving MAFLD. Although some studies have analyzed the effect of CR on MAFLD, there are few studies related to TRF and MAFLD, in particular, studies comparing the effects of TRF and CR are lacking [7].

Therefore, in this study, we analyzed the efficacy of TRF and CR in MAFLD, and also combined these strategies to simultaneously observe the effects of restricted eating time and food intake. This provides both a clinical and theoretical reference point for MAFLD prevention and treatment. Finally, based on the results of liver metabolomics, we studied the *peroxisome proliferator-activated receptor alpha* (PPAR α) and *silent information regulator* (SIRT1) genes related to the PPAR signaling pathway to clarify the relevant mechanisms in this study [8, 9].

Materials and methods

Animals and the study protocol

Fifty specific-pathogen-free male Sprague–Dawley rats were raised at the Animal Center of Xi'an Jiaotong University (license No. SYXK (Shaanxi) 2020–005). The living conditions included a day-to-night ratio of 12:12 h, a temperature of 22 °C, and free access to water. After 1 week of adaptive feeding and using a random number table method, 12 animals were assigned to the Normal group and given an ordinary diet (the carbohydrate, protein, and fat energy accounted for 65%, 25%, and 10%, respectively. Xi'an Jiaotong University, Xi'an, China). The remaining 38 animals (MAFLD group) were fed a

high-fat diet (the carbohydrate, protein, and fat energy accounted for 20%, 20%, and 60%, respectively. SYSE BIO, Changzhou, China). The high-fat diet was purchased from Changzhou SYSE BIO (China); At 10 weeks, two rats were randomly selected from the MAFLD group, and livers were removed for hematoxylin and eosin (HE) staining to ensure MAFLD in rats induced by a high-fat diet for 10 weeks [10]. Then, the remaining 36 rats were randomly divided into four groups of nine animals/group: the 4 h TRF group (feeding at 18:00–22:00), the 60% CR group (Normal group rats with the standard-food intake/unit body weight calculated as 60%), the 4 h TRF + 60% CR group (feeding at 18:00–22:00 and a 40% calorie intake reduction), and the Model group (free eating). During the intervention period from weeks 11 to 14, body weight was measured weekly, and food intake was assessed daily in the four groups. Our study was approved by the Biomedical Ethics Committee of Xi'an Jiaotong University Health Science Center (XJTUAE2023-1434).

Serum biochemical indicators

At the end of 14 weeks, after fasting overnight for 12 h, the rats were anesthetized via intraperitoneal injection of 1% pentobarbital sodium (50 mg/kg). Then, 4 mL of blood was collected from the heart, left for 1 h at room temperature, and centrifuged for 10 min at 3500 rpm, after which the serum was separated. Fasting blood glucose (FBG), total cholesterol (TC), triglyceride (TG), low-density lipoprotein (LDL), high-density lipoprotein (HDL), alanine aminotransferase (ALT), and aspartate aminotransferase (AST) levels were measured using an automatic biochemical analyzer (Beckman Coulter, CA, USA). The body fat ratio was defined as (epididymis fat + perirenal fat)/weight \times 100%.

Pathological histology

For HE staining, approximately 5 mm of liver tissue was fixed in 4% paraformaldehyde, dehydrated, paraffin-embedded, sliced, and stained with HE. Oil red staining, approximately 5 mm liver tissue was fixed in 4% paraformaldehyde, dehydrated, optimal cutting temperature compound (OCT, Sakura, Tokyo, Japan) embedded, sectioned, stained, glycerin gelatin tablet (Servicebio, Wuhan, China) sealed. Pathological changes across groups were observed via microscopy (Nikon, Tokyo, Japan). ImageJ software (v1.8.0; National Institutes of Health, Bethesda, USA) was used to calculate the area occupied by fat droplets, which represented the liver fat content.

Metabolomics

Liver tissue was homogenized in a grinder (30 Hz; Leica Biosystems, Shanghai, China) for 20 s. A 400 μ L solution

(methanol: water=7:3, V/V) containing an internal standard was added to 20 mg of ground tissue and shaken at 1500 rpm for 5 min. After being placed on ice for 15 min, the tissue was centrifuged at 12,000 rpm for 10 min (4 °C). Then, 300 μ L of the supernatant was incubated at -20°C for 30 min and centrifuged at 12,000 rpm for 3 min (4 °C), after which 200 μ L of the sample was processed using liquid chromatography with electrospray ionization tandem mass spectrometry (SCIEX, CA, USA). Principal component analysis (PCA), orthogonal partial least squares discriminant analysis (OPLS-DA), Kyoto Encyclopedia of Genes and Genomes (KEGG) database was used to annotate and display the differential metabolites and analyze the related metabolic pathways [11].

Real-time polymerase chain reaction (RT-PCR)

Total RNA of liver tissue was extracted using a Total RNA Extraction Kit I, and the RNA concentrations were determined via spectrophotometry (NanoDrop, Thermo Fisher Scientific, Waltham, MA, USA). Total RNA was transcribed to cDNA using PrimeScript RT Master Mix (TaKaRa, Shiga, Japan) and TB Green Premix Ex Taq II kits (TaKaRa, Shiga, Japan). ABI StepOne Plus (Thermo, CA, USA) was used to determine the relative abundance of the mRNAs. All procedures were conducted in accordance with the manufacturer's instructions. Gene expression was quantified using the $2^{-\Delta\Delta C_t}$ method. The following primers were used: *PPAR α* (Augct, Beijing, China); the upstream primer TCTGAACATTGGCGTTCGCAG; the downstream primer CTCGTGTGCCCTCCCTCAAG; the *SIRT1* (Augct) upstream primer GGCAGACAATTTAATGGGGTGA; the downstream primer ATCTGGGAGATCCGGGAAGT; the *GAPDH* (Augct) upstream primer TACCCACGGCAAGTTCAACG; and the downstream primer CACCAGCATCACCCATT

TG. *GAPDH* was used as internal reference gene to calculate the relative expression of target gene.

Statistical analyses

Normal data are expressed as the mean \pm standard deviation. One-way analysis of variance was initially used, after which Fisher's least significant difference (LSD) test or Tamhane T2 test was used to determine statistical significance. Skewness data were described by quartile spacing and compared using the Kruskal–Wallis test. IBM SPSS 23.0 statistical software (SPSS, Inc., Armonk, NY, USA) was used for the statistical analyses. GraphPad Prism 8.0 software (San Diego, CA, USA) was used to generate graphs. A $p < 0.05$ indicated statistical significance.

Results

The effects of 4 h TRF and 60% CR on body weight and body fat in MAFLD rats

On the 10th weekend, two rats in the MAFLD group were randomly selected and HE staining of liver tissues showed that hepatocytes were swollen, with many lipid droplets of various sizes present in hepatocytes. In addition, some nuclei were compressed and displaced (Fig. 1). The body weight of the rats in the Normal group and the MAFLD group increased gradually. By the end of week 10, the body weight of the rats in the Normal and the MAFLD group were 393.8 ± 35.8 g and 470.4 ± 53.4 g, respectively. This difference was statistically significant ($p < 0.001$; Fig. 2a), indicating successful construction of the MAFLD model.

At the end of 14 weeks, the body weight of the Normal, TRF, CR, TRF+CR, and Model groups were 419.1 ± 41.0 g, 418.0 ± 36.0 g, 413.3 ± 53.6 g, 388.6 ± 45.8 g and 477.9 ± 37.9 g, respectively. The differences were statistically significant ($P = 0.002$). Body weight was lower in the Normal, TRF, CR, and TRF+CR groups than in the

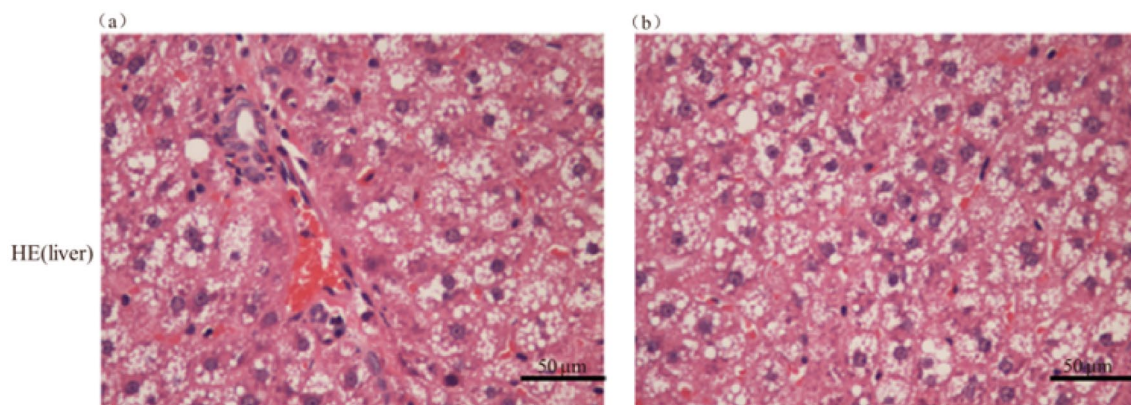


Fig. 1 Establishment of MAFLD rat model. At the end of 10 weeks, HE liver tissue staining confirmed successful MAFLD model construction (400 \times magnification)

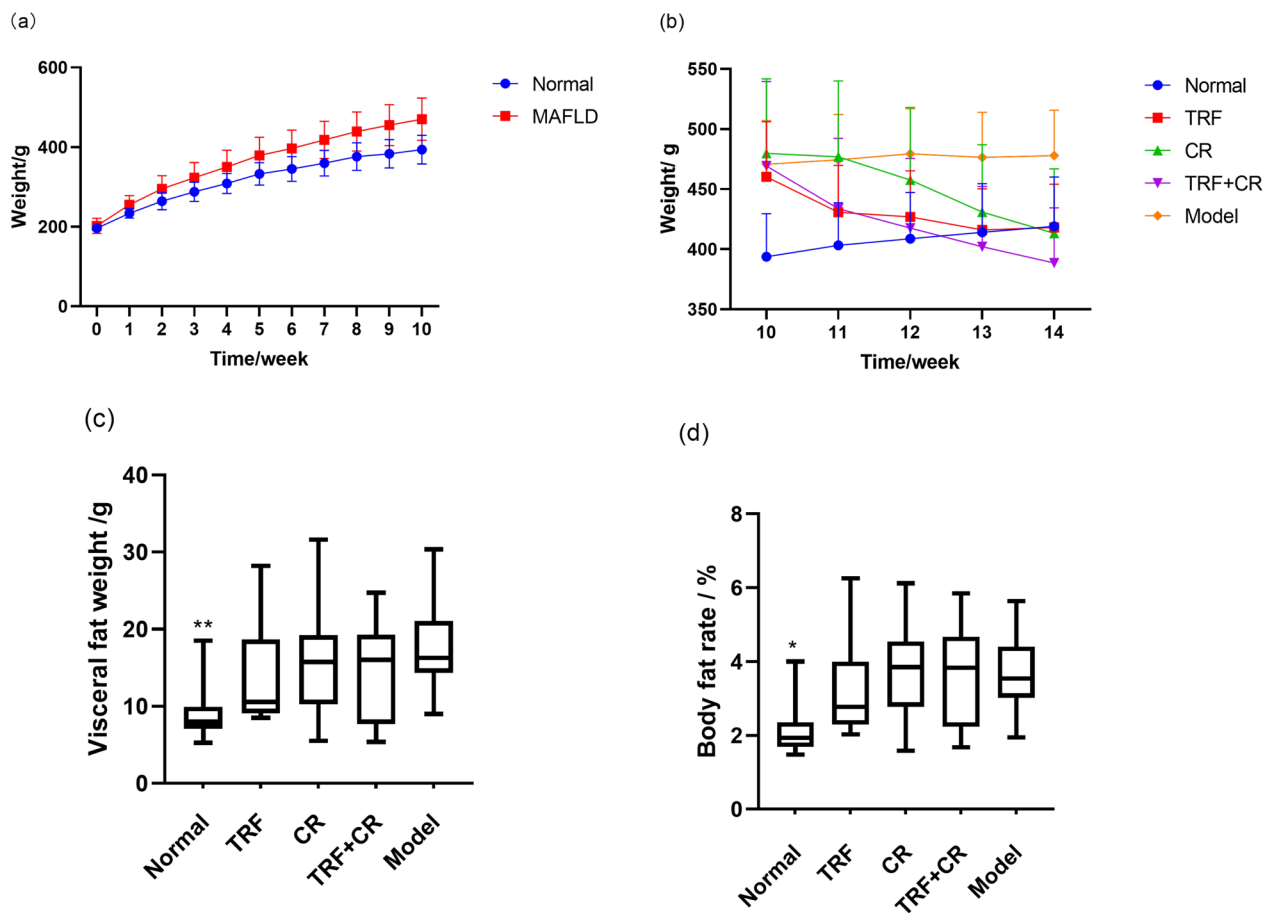


Fig. 2 Body weight and body fat parameters in MAFLD rats. **a** Body weight (g) at weeks 1–10; **b** weight (g) at 11–14 weeks; **c** perirenal fat and epididymal fat weight (g); **d** body fat ratios (%). The data are presented as the mean \pm standard deviation or percentile spacing. Compared with the Model group, * $p < 0.05$, ** $p < 0.01$. Normal, rats fed a normal diet ad libitum; TRF, feeding at 18:00–22:00; CR, a 40% calorie intake reduction; TRF + CR, feeding at 18:00–22:00 and a 40% calorie intake reduction; Model, free eating

Model group ($p < 0.01$; Fig. 2b). The visceral fat weight and body fat ratios were significantly different among the Normal, TRF, CR, TRF + CR, and Model groups ($p < 0.05$; Fig. 2c–d). The visceral fat weight and body fat ratio in the Normal group were the lowest in the five groups, but there were significant differences than that in the Model ($p < 0.01$, $p < 0.05$; Fig. 2c–d).

The effects of 4 h TRF on food intake in MAFLD rats

In the first week of treatment, the food intake in the Normal, CR, and Model groups was relatively stable, while the food intake in the TRF and TRF + CR groups was relatively low during the first two days of TRF (Fig. 3a). The food intake on the third day significantly increased.

In weeks 11–14, the food intake in the Normal group was stable (Fig. 3b). The food intake in the TRF group was low in the first week and then increased, and it was low in the TRF + CR group in the first week and was basically stable by the second week. The food intake in the

Model group gradually increased and stabilized in week 3.

The average food intake levels in the Normal, TRF, CR, TRF + CR, and Model groups were 24.9 ± 1.5 g, 17.7 ± 5.0 g, 16.9 ± 1.4 g, 13.2 ± 2.9 g, and 24.0 ± 2.6 g, respectively, with significant differences observed during weeks 11–14 ($p < 0.001$). No statistically significant differences were observed between the Normal group and Model group, or between CR group and TRF group ($p > 0.05$), but statistically significant differences in average daily food intake were observed among the other groups ($p < 0.01$). Compared with the Normal group, 4 h TRF reduced about 29% of daily food intake.

Effects of 4 h TRF and 60% CR on biochemical indices

There were no significant differences in serum ALT, AST, FBG, TC, HDL, and LDL levels between the groups ($p > 0.05$; Fig. 4).

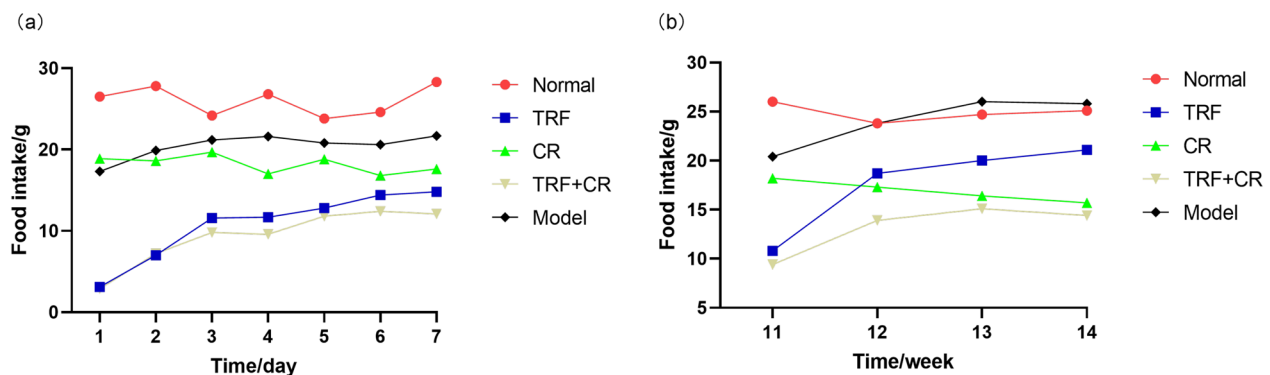


Fig. 3 Average daily food intake of MAFLD rats. **a** Daily average food intake (g) in rats for days 1–7. **b** Average food intake from week 11–14 (g). Average daily food intake = total food intake in each group/number of rats per group. Normal, rats fed a normal diet ad libitum; TRF, feeding at 18:00–22:00; CR, a 40% calorie intake reduction; TRF + CR, feeding at 18:00–22:00 and a 40% calorie intake reduction; Model, free eating

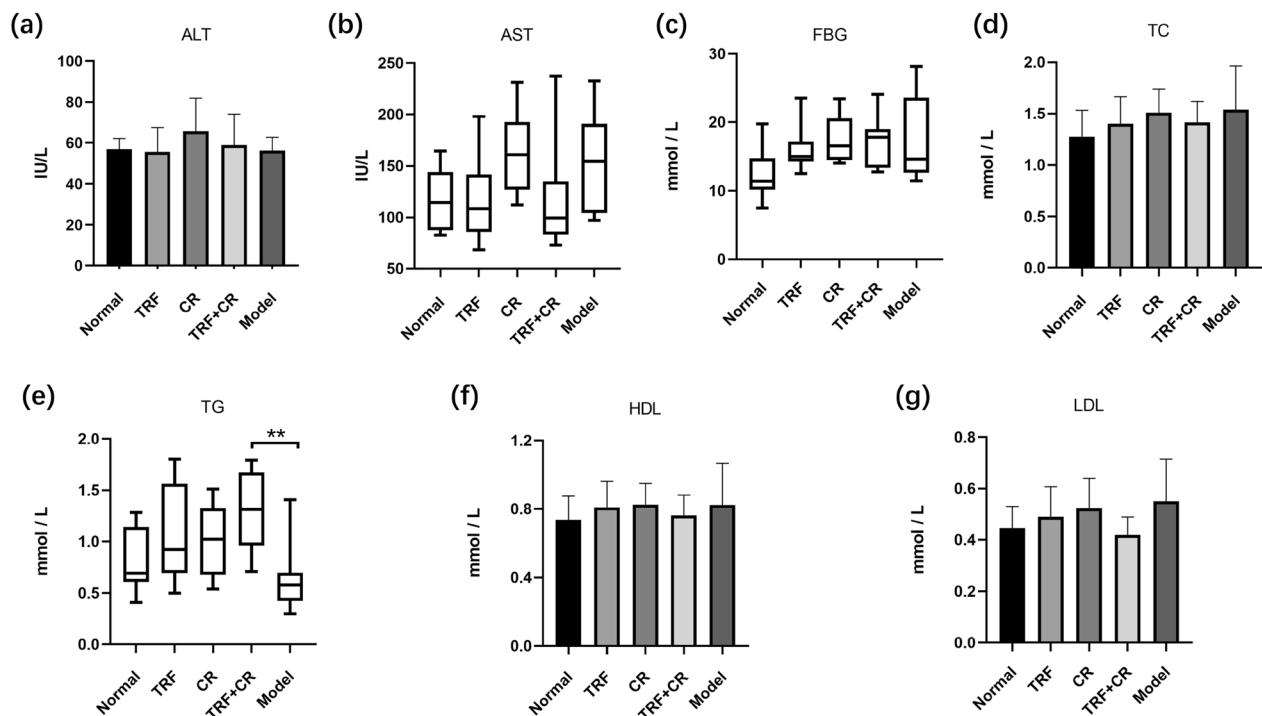


Fig. 4 Serum biochemical indices of MAFLD rats. At the end of 14 weeks, Serum biochemical indices including ALT (**a**), AST (**b**), FBG (**c**), TC (**d**), TG (**e**), HDL (**f**) and LDL (**g**), which were measured using an automatic biochemical analyzer. Results were presented as the mean \pm standard deviation or percentile spacing. Compared with the Model group, * $p < 0.05$, ** $p < 0.01$. Normal, rats fed a normal diet ad libitum; TRF, feeding at 18:00–22:00; CR, a 40% calorie intake reduction; TRF + CR, feeding at 18:00–22:00 and a 40% calorie reduction; Model, free eating

TG levels were significantly different among the five groups ($p < 0.05$), and its levels in the TRF + CR group were significantly higher than those in the Model group ($p < 0.01$), and there were no significant differences among the other groups ($p > 0.05$; Fig. 4e).

Pathology of liver tissue and adipose tissue

After adjusting the diet structure, replacing the high-fat diet with an ordinary diet (10% low-fat diet, 11–14 weeks), the structure of the liver cord was normal and radially arranged, the morphology of the hepatocytes

was not abnormal, and no obvious lipid droplets were observed in the Normal group. The results for the TRF, the CR and the TRF+CR groups were similar to those for the Normal group (Fig. 5a–e). However, the rat hepatocytes in the Model group still contained a small amount of lipid droplets (Fig. 5f–j). Oil red O staining of liver tissue was quantified by ImageJ software and the liver fat levels in the other four groups were lower than those in the Model group ($p < 0.05$; Fig. 6). The liver fat content in the TRF+CR group was lower than that in the Normal and Model groups ($p < 0.05$; Fig. 6).

In addition, we also observed the adipocytes were arranged neatly and evenly in the Normal, TRF, CR, and TRF+CR groups, while the adipocytes were different in size, larger in volume, and more disordered in the Model group (Fig. 5k–o).

Liver metabolomics

To explore the mechanism through which TRF and CR improve MAFLD, liver metabolomics was conducted in our study. An orthogonal partial least squares discriminant analysis (OPLS-DA) score chart and model verification results confirmed the validity of our model. Our extensive and targeted metabolomics detected 1290 metabolites. Compared with those in the Normal group, 367 metabolites, including 12(S)-hydroxy-(5Z,8Z,10E,14Z)-eicosatetraenoic acid, arachidonic acid, and glucuronic acid, were elevated in the Model group, while 105 metabolites, including adenosine diphosphate and uracil-diphosphate glucose, were

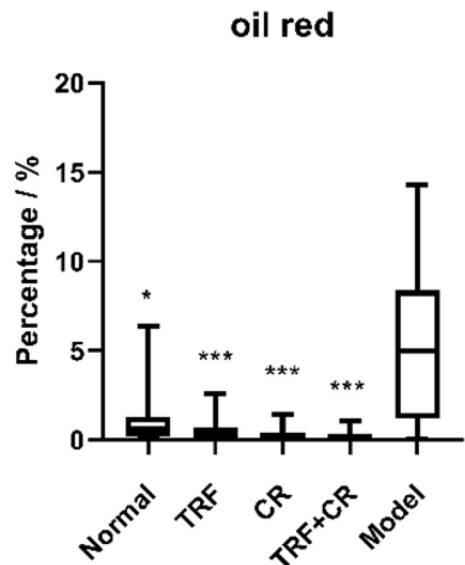


Fig. 6 Semi-quantitative oil red O staining results in liver tissue. The data are represented as the mean \pm standard deviation. Compared with the Model group, * $p < 0.05$ and *** $p < 0.001$. Normal, rats fed a normal diet ad libitum; TRF, feeding at 18:00–22:00; CR, a 40% calorie intake reduction; TRF + CR, feeding at 18:00–22:00 and a 40% calorie intake reduction; Model, free eating

decreased (Fig. 7). Compared with those in the Model group, 110 metabolites, such as (\pm) 12(S)-hydroxy-(5Z,8Z,10E,14Z)-eicosatetraenoic acid, were decreased in the TRF+CR group, and 83 metabolites, such as LysoPC (14:0/0:0) which was a lysophospholipid and

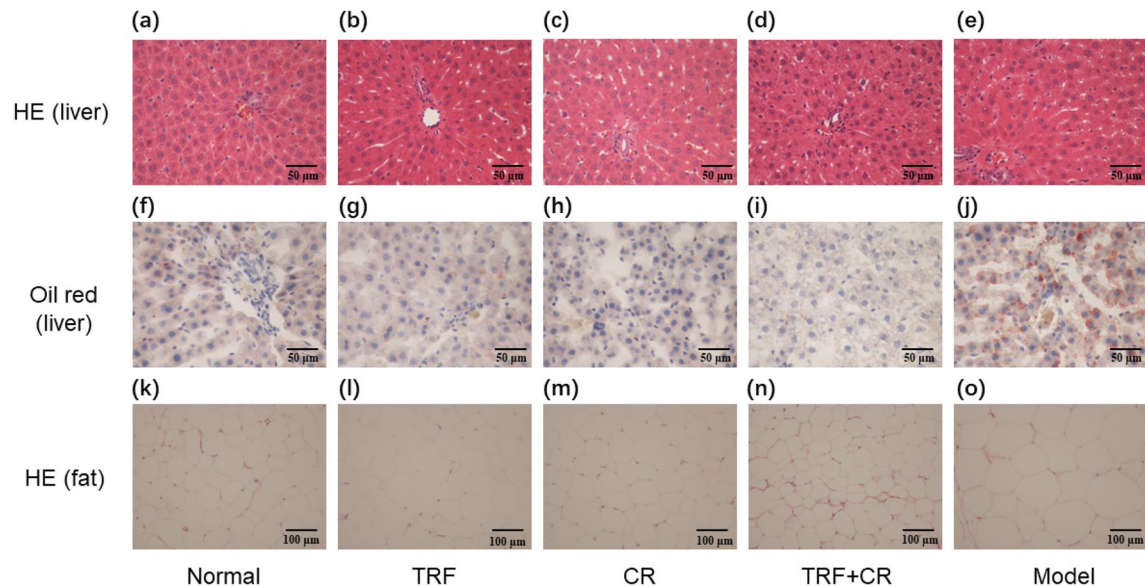


Fig. 5 Pathological findings in MAFLD rats. Rat liver tissue was stained with HE (400 \times magnification), liver oil red O (400 \times magnification) and perirenal fat (200 \times magnification). Scale bar = 50/100 μ m. Normal, rats fed a normal diet ad libitum; TRF, feeding at 18:00–22:00; CR, a 40% calorie intake reduction; TRF + CR, feeding at 18:00–22:00 and a 40% calorie intake reduction; Model, free eating

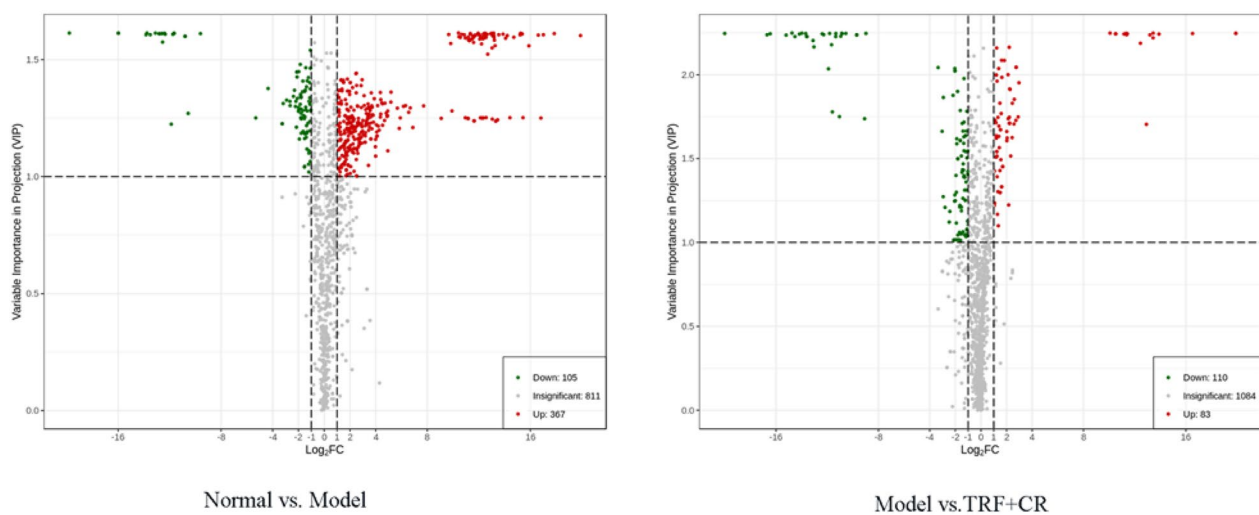


Fig. 7 Metabolomics map. Volcanic map showing differentially abundant metabolites. Each dot in the volcanic map represents a metabolite, while the green, red, and gray dots represent decreased, elevated, and nonsignificant metabolites, respectively. The horizontal coordinate represents the inverse value of the multiple differences in the relative content of metabolites in the liver of rats in the different groups (\log_2FC). Normal, rats fed a normal diet ad libitum; TRF, feeding at 18:00–22:00; CR, a 40% calorie intake reduction; TRF + CR, feeding at 18:00–22:00 and a 40% calorie intake reduction; Model, free eating

PC (12:0/12:0) which was phosphatidylcholine, were elevated (Fig. 7).

According to the original relative content of differentially abundant metabolites, a heatmap was drawn to observe the change in the relative content of metabolites (Fig. 8a–b), and a Venn diagram was generated to show the relationship between the different metabolites of each group (Fig. 8c). The heat maps of one of the rats in the Model group were similar to those of the Normal group, but the remaining three were significantly different, which may be caused by differences in the population.

KEGG pathway enrichment analysis of the different metabolites in the different groups was performed to determine the mechanism related to lipid clearance in the liver. The main pathways identified in the comparison of the Normal group and the Model group included PPAR signaling, adenosine 5'-monophosphate (AMP)-activated protein kinase (AMPK) signaling and so on (Fig. 9a). We observed that the related mechanisms involved arachidonic acid metabolism, the digestion and absorption of carbohydrates, and so on, when compared with those in the Model and TRF + CR groups (Fig. 9b).

The effects of 4 h TRF and 60% CR on liver lipid metabolism genes

Based on the KEGG pathway enrichment results, we investigated the *PPARα* and *SIRT1* genes, which are related to the PPAR signaling pathway, to further explore liver lipid metabolism-related mechanisms. The *PPARα* mRNA levels were increased in the CR, Model

groups and there was no significant difference among the five groups (Fig. 10). The *SIRT1* mRNA levels were different among the five groups ($P=0.003$; Fig. 10). Compared with those in the Normal group, the *SIRT1* mRNA levels were significantly higher in the other four groups, but only the CR and Model groups were significantly different ($p < 0.05$; Fig. 10). Therefore, the *PPARα* and *SIRT1* mRNA levels in the TRF + CR group were lower than those in the TRF, CR, and Model groups, but the differences were not statistically significant ($p > 0.05$).

Discussion

MAFLD can be completely reversed by early treatment, but without timely intervention, it may progress to hepatitis, cirrhosis and liver cancer [12, 13]. However, there is a dearth of specific therapeutics available for treating MAFLD [14]. Currently, first-line treatments for MAFLD mainly focus on improving lifestyles by adjusting diets and increasing exercise levels [15, 16]. There are many studies on CR improving MAFLD, but for most people, counting calories in food is challenging [17]. Counting calories is hard, but reducing caloric intake is even harder. In recent years, more and more scholars have begun to pay attention to TRF, which may improve MAFLD [18].

TRF may reduce weight and ameliorate metabolic disorders, and may be used to improve MAFLD, but its specific role and mechanism of action are still unclear. A previous basic experiment showed that 8 h TRF reduced food intake and reversed high-fat diet-induced

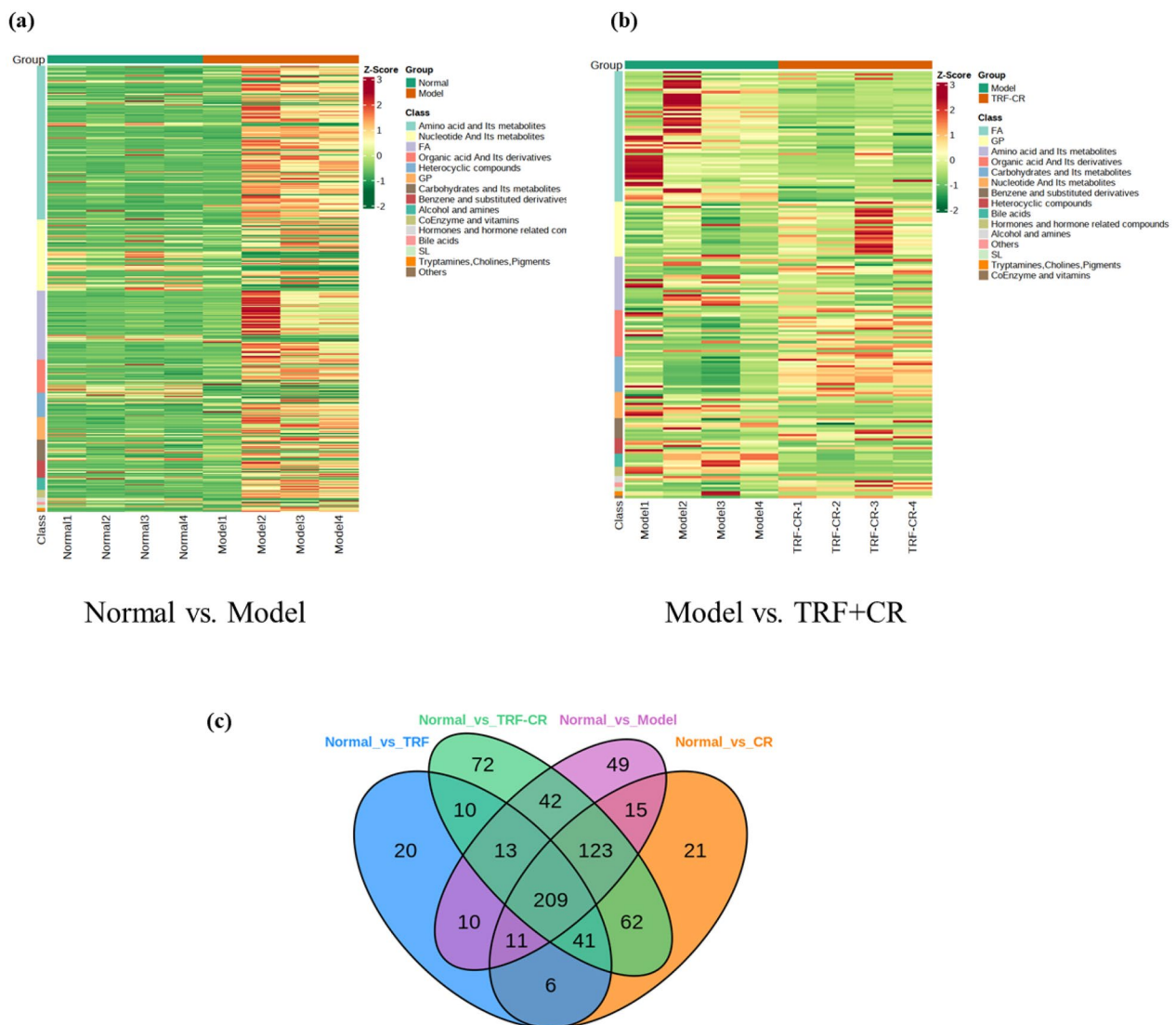


Fig. 8 Heatmap and Venn diagram. **a, b** Cluster heatmap showing differentially abundant metabolites. The horizontal and vertical axes are the sample name and differentially abundant metabolite information, respectively. Red and green indicate high and low contents, respectively; **c** Venn diagram showing differentially abundant metabolites. Each circle in the figure represents a group, numbers with no overlap represent the number of unique differentially abundant metabolites, and numbers with overlap represent the number of shared differentially abundant metabolites. Normal, rats fed a normal diet ad libitum; TRF, feeding at 18:00–22:00; CR, a 40% calorie intake reduction; TRF + CR, feeding at 18:00–22:00 and a 40% calorie intake reduction; Model, free eating

hyperglycemia and insulin resistance in a high-fat diet-induced obese mouse [19]. Other studies reported that TRF improved obesity and prevented liver steatosis in young adolescent obese mice [20]. Our previous study suggested that TRF improve MAFLD via reducing food intake by 13% and improving the expression of genes in the PPAR α /FAS pathway [21]. A survey of dietary and demographic data from adult subjects showed that the 10 h TRF was negatively correlated with overweight/obesity and dyslipidemia, while 8 h TRF was associated with only overweight/obesity but not type 2 diabetes mellitus

[22], different eating times may have different effects. In addition, specific time for restricted feeding and circadian rhythm are also important [23].

Therefore, we simulated improvements in diet structure and further restricted eating time, the therapeutic effects of 4 h TRF and 60% CR on MAFLD were analyzed for the first time, and 4 h TRF + 60% CR treatments were combined to observe their therapeutic effects. Body weight did not significantly change, but liver lipid content decreased after the consumption of an ordinary diet in high-fat diet induced-MAFLD rats. However, both

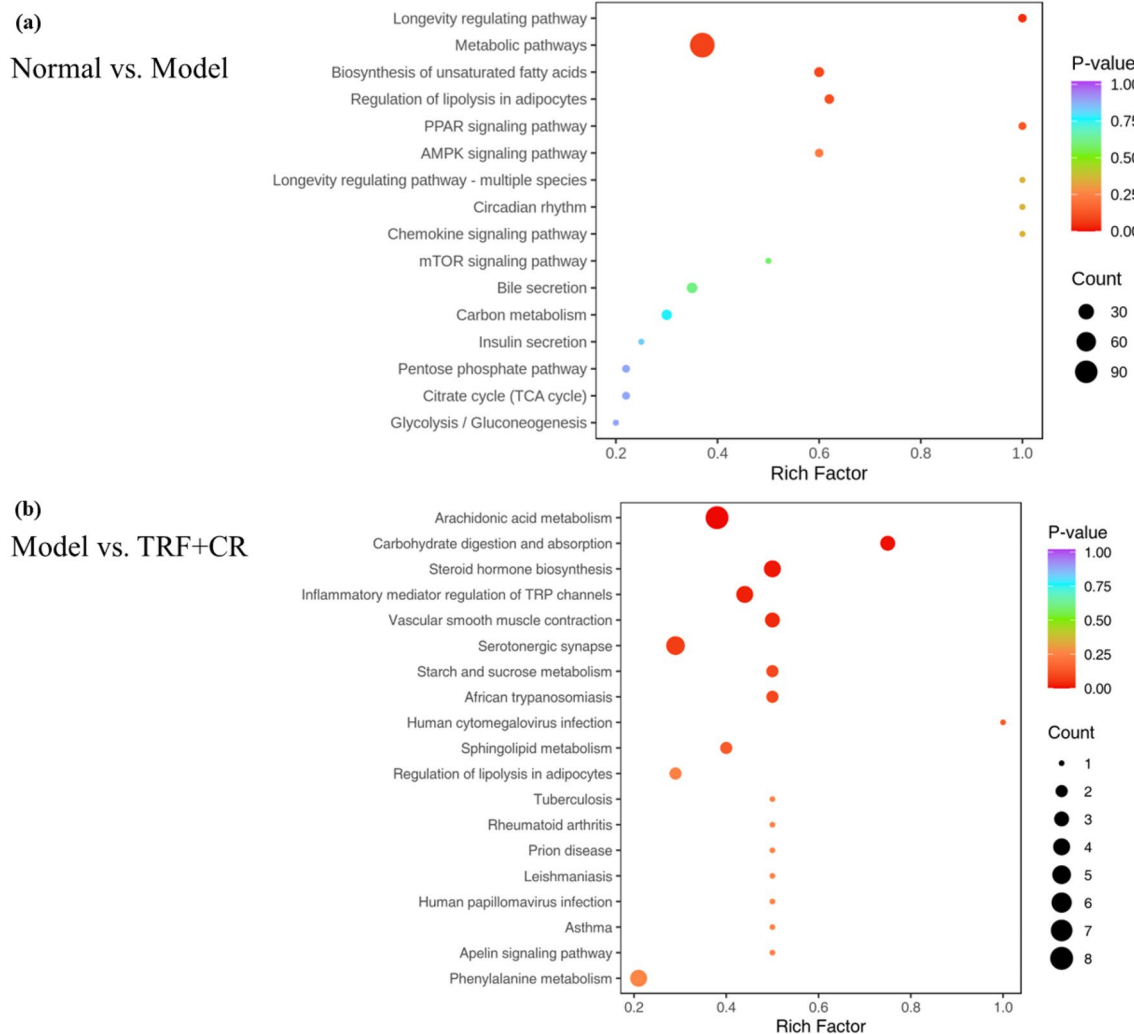


Fig. 9 KEGG pathway enrichment analysis. KEGG pathway enrichment based on the results of differentially abundant metabolites in liver tissue. The abscissa represents the Rich factor corresponding to each pathway, the ordinate represents the pathway name, and the color of the dots indicates the *P* value: the redder the point is, the more significant the enrichment. The size of the dot represents the number of enriched differentially abundant metabolites. Normal, rats fed a normal diet ad libitum; TRF, feeding at 18:00–22:00; CR, a 40% calorie intake reduction; TRF + CR, feeding at 18:00–22:00 and a 40% calorie intake reduction; Model, free eating

4 h TRF and 60% CR significantly reduced body weight and liver lipid content without significantly increase serum TG levels. Then, the body weight reductions in the TRF+CR group were more obvious and this combined treatment significantly increased the serum TG concentration, possibly through excessive weight loss and fat decomposition. In addition, the rat hepatocytes in the Model group still contained a small amount of lipid droplets and the liver fat levels that was used by oil red O staining in the other four groups were lower than those in the Model group. These results revealed that the liver fat levels were decreased by 4 h TRF and 60% CR. At the same time, we found that 4 h TRF limited approximately

29% of the average daily food intake. In conclusion, we investigated that both 4 h TRF and 60% CR can alleviate MAFLD rats by reducing body weight, food intake, and liver fat content. While 4 h TRF was similar but superior to CR, it was superior in restricting both eating times and caloric intake. Importantly, we do not recommend the combination treatment of 4 h TRF and CR on 60% MAFLD, this can lead to excessive fat breakdown and elevated serum triglyceride levels.

Previous studies have confirmed that PPAR α , SIRT1 and other molecules are closely related to lipid metabolism [24, 25]. PPAR α is a member of the nuclear receptor superfamily and excessive fat intake can reduce the

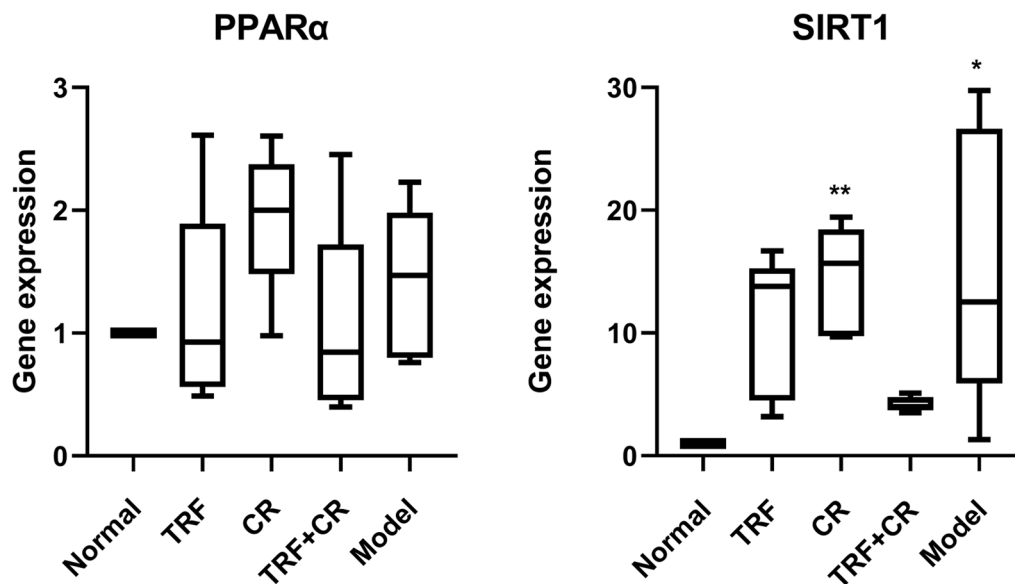


Fig. 10 Gene expression related to liver lipid metabolism. At the end of 14 weeks, all rats were humanely sacrificed, and liver tissue was extracted. *PPARα* and *SIRT1* mRNA levels were determined via real-time PCR. The data are represented by the percentile spacing. Comparisons were made to the Normal group, * $p < 0.05$, ** $p < 0.01$. Normal, rats fed a normal diet ad libitum; TRF, feeding at 18:00–22:00; CR, a 40% calorie intake reduction; TRF + CR, feeding at 18:00–22:00 and a 40% calorie intake reduction; Model, free eating

expression of *PPARα* to form MAFLD. *PPARα* upregulation promotes β -oxidation of free fatty acid, reduces TG and fat production in the liver, and improves MAFLD [26, 27]. *SIRT1* is one of the most important and widely studied members of sirtuins and is considered to play an important role in metabolic regulation, longevity and so on [28]. *SIRT1* improves MAFLD by proliferator-activated receptor gamma coactivator-1 alpha (PGC-1 α) deacetylation. In this study, KEGG analysis indicated that lipid clearance in the liver involved *PPAR* signaling, AMPK signaling, metabolic pathways and so on. Based on KEGG enrichment data, *PPAR* signaling pathway-related genes *PPARα* and *SIRT1* were examined to characterize the underlying mechanisms. We found that the *SIRT1* and *PPARα* mRNA levels in the other four groups were increased when compared with those in the Normal group, but there was no significant difference between some groups. The *PPARα* and *SIRT1* mRNA levels in the TRF + CR group were lower than those in the TRF, CR, and Model groups, but the differences were not statistically significant. This observation may be related to differences in liver lipid content in rats at different time points or the limited sample size in our study. While our findings confirmed the benefits of 4 h TRF, other studies suggested that these benefits may be limited. For example, a Chinese study reported that 8 h TRF was no more effective for weight loss than a CR regimen and no significant differences in weight

change [23], different eating times may have different effects, and more research is needed to compare them.

In this study, the effects of 4 h TRF and 60% CR on MAFLD rats were compared for the first time, and TRF and CR were combined to observe the effects of limiting food intake and eating time at the same time. We also discussed the potential mechanisms underlying these effects. Finally, some valuable results are obtained, after the high-fat diet was discontinued, the lipid of the liver in the rat with MAFLD significantly reduced, the weight was not significantly changed. We observed that the 4 h TRF, 60% CR, and 4 h TRF + 60% CR regimens significantly reduced the body weight and liver lipid content of MAFLD rats. However, the 4 h TRF + 60% CR approach led to excessive weight loss and fat decomposition, significantly increased serum TG levels. 4 h TRF improved MAFLD without excessive food intake restriction, thereby providing a new strategy and basis for the clinical transformation of MAFLD using TRF approaches.

Although these findings are valuable, this was an animal study in which the rats were forced to limit the amount of food intake or eating times for therapeutic purposes. However, in real life, how people comply with these interventions still needs to be further studied through clinical trials, which is a focus of our ongoing research. Additionally, further studies are required to compare the effects of TRF and CR in rats on a high-fat

diet, and to better understand the mechanism of lipid clearance after the high-fat diet is discontinued.

Author contributions

Jiang Deng and Xin Zhang conceived and designed the study. Kairuo Wang and Juan Ma performed the animal experiments. Yikai Wang and Ning Gao were responsible for data collection and analysis. Dandan Feng and Xiaoli Jia contributed to the interpretation of the data. Xiongtao Liu provided technical assistance. Shuangsoo Dang and Juanjuan Shi supervised the project and revised the manuscript. All authors contributed to manuscript preparation, read, and approved the final version.

Funding

The Key Research and Development Program of Shaanxi, No. 2021SF- 227.

Data availability

No datasets were generated or analysed during the current study.

Declarations

Consent for publication

All participants in this study have agreed to publish it.

Ethical approval

This study was approved by the Biomedical Ethics Committee of Xi'an Jiaotong University Health Science Center (XJTUAE2023-1434).

Conflict of interest

The authors declare no competing interests.

Author details

¹Department of Gastroenterology, The Second Affiliated Hospital of Xi'an Jiaotong University, Xi'an, China. ²Department of Infectious Disease, The Second Affiliated Hospital of Xi'an Jiaotong University, Xi'an 710004, China. ³Department of Operating Room, The Second Affiliated Hospital of Xi'an Jiaotong University, Xi'an, China.

Received: 17 October 2024 Accepted: 6 February 2025

Published online: 19 February 2025

References

- Trajkovska Petkoska A, Trajkovska-Broach A. Mediterranean diet: a nutrient-packed diet and a healthy lifestyle for a sustainable world. *J Sci Food Agric*. 2021;101:2627–33.
- Zhou F, Zhou J, Wang W, Zhang XJ, Ji YX, Zhang P, She ZG, Zhu L, Cai J, Li H. Unexpected rapid increase in the burden of NAFLD in China from 2008 to 2018: a systematic review and meta-analysis. *Hepatology*. 2019;70:1119–33.
- Younossi ZM, Golabi P, Paik JM, Henry A, Van Dongen C, Henry L. The global epidemiology of nonalcoholic fatty liver disease (NAFLD) and nonalcoholic steatohepatitis (NASH): a systematic review. *Hepatology*. 2023;1(77):1335–47.
- Guo Y, Livelio C, Melkani GC. Time-restricted feeding regulates lipid metabolism under metabolic challenges. *BioEssays*. 2023;45: e2300157.
- Li G, Xie C, Lu S, Nichols RG, Tian Y, Li L, Patel D, Ma Y, Brocker CN, et al. Intermittent fasting promotes white adipose browning and decreases obesity by shaping the gut microbiota. *Cell Metab*. 2017;3(26):672–85. e4.
- Sun Y, Ye Y, He Y, Liu S. Time-restricted feeding: what we have done and what more we can do? *Hepat Surg Nutr*. 2023;1(12):440–2.
- Minciuna I, Gallage S, Heikenwalder M, Zelber-Sagi S, Dufour JF. Intermittent fasting-the future treatment in NASH patients? *Hepatology*. 2023;1(78):1290–305.
- Cantó C, Auwerx J. PGC-1 α , SIRT1 and AMPK, an energy sensing network that controls energy expenditure. *Curr Opin Lipidol*. 2009;20:98–105.
- Qian L, Zhu Y, Deng C, Liang Z, Chen J, Chen Y, Wang X, Liu Y, Tian Y, Yang Y. Peroxisome proliferator-activated receptor gamma coactivator-1 (PGC-1) family in physiological and pathophysiological process and diseases. *Signal Transduct Target Ther*. 2024;1(9):50.
- Wu L, Mo W, Feng J, Li J, Yu Q, Li S, Zhang J, Chen K, Ji J, et al. Astaxanthin attenuates hepatic damage and mitochondrial dysfunction in non-alcoholic fatty liver disease by up-regulating the FGF21/PGC-1 α pathway. *Br J Pharmacol*. 2020;177:3760–77.
- Hou C, Huang M, Wang P, Zhang Q, Wang G, Gao S. Chronic exposure to 3,6-dichlorocarbazole exacerbates non-alcoholic fatty liver disease in zebrafish by disrupting lipid metabolism and inducing special lipid biomarker accumulation. *Chemosphere*. 2024;352: 141442.
- Peiseler M, Tacke F. Inflammatory mechanisms underlying Nonalcoholic Steatohepatitis and the transition to hepatocellular carcinoma. *Cancers*. 2021;10:13.
- Sangro P, de la Torre AM, Sangro B, D'Avola D. Metabolic dysfunction-associated fatty liver disease (MAFLD): an update of the recent advances in pharmacological treatment. *J Physiol Biochem*. 2023;79:869–79.
- Zhao Y, Zhou Y, Wang D, Huang Z, Xiao X, Zheng Q, Li S, Long D, Feng L. Mitochondrial dysfunction in metabolic dysfunction fatty liver disease (MAFLD). *Int J Mol Sci*. 2023;15:24.
- Keating SE, Sabag A, Hallsworth K, Hickman IJ, Macdonald GA, Stine JG, George J, Johnson NA. Exercise in the management of metabolic-associated fatty liver disease (MAFLD) in adults: a position statement from exercise and sport science Australia. *Sports Med*. 2023;53:2347–71.
- Damasceno de Lima R, Fudoli Lins Vieira R, Rosetto Muñoz V, Chaix A, Azevedo Macedo AP, Calheiros Antunes G, Felonato Rosseto Braga MR, Nakandakari CBRS, et al. Time-restricted feeding combined with resistance exercise prevents obesity and improves lipid metabolism in the liver of mice fed a high-fat diet. *Am J Physiol Endocrinol Metab*. 2023;1(325):E513–28.
- Hadeifi A, Arvanitakis M, Trépo E, Zelber-Sagi S. Dietary strategies in non-alcoholic fatty liver disease patients: From evidence to daily clinical practice, a systematic review. *United European Gastroenterol J*. 2023;11:663–89.
- Mentzelou M, Papadopoulou SK, Psara E, Voulgaridou G, Pavlidou E, Androutsos O, Giaginis C. Chrononutrition in the prevention and management of metabolic disorders: a literature review. *Nutrients*. 2024;1:16.
- She Y, Sun J, Hou P, Fang P, Zhang Z. Time-restricted feeding attenuates gluconeogenic activity through inhibition of PGC-1 α expression and activity. *Physiol Behav*. 2021;15(231): 113313.
- Ribas-Aulinas F, Parra-Vargas M, Ramon-Krauel M, Diaz R, Lerin C, Cambras T, Jimenez-Chillaron JC. Time-restricted feeding during puberty ameliorates adiposity and prevents hepatic steatosis in a mouse model of childhood obesity. *Nutrients*. 2021;13:13.
- Deng J, Feng D, Jia X, Zhai S, Liu Y, Gao N, Zhang X, Li M, Lu M, et al. Efficacy and mechanism of intermittent fasting in metabolic associated fatty liver disease based on ultraperformance liquid chromatography-tandem mass spectrometry. *Front Nutr*. 2022;9: 838091.
- Currenti W, Buscemi S, Cincione RI, Cernigliaro A, Godos J, Grosso G, Galvano F. Time-restricted feeding and metabolic outcomes in a cohort of Italian adults. *Nutrients*. 2021;13:13.
- Liu D, Huang Y, Huang C, Yang S, Wei X, Zhang P, Guo D, Lin J, Xu B, et al. Calorie Restriction with or without time-restricted eating in weight loss. *N Engl J Med*. 2022;21(386):1495–504.
- Shen S, Shen M, Kuang L, Yang K, Wu S, Liu X, Wang Y, Wang Y. SIRT1/SREBPs-mediated regulation of lipid metabolism. *Pharmacol Res*. 2024;199: 107037.
- Kuang J, Wang J, Li Y, Li M, Zhao M, Ge K, Zheng D, Cheung KCP, Liao B, et al. Hydoxycholeic acid alleviates non-alcoholic fatty liver disease through modulating the gut-liver axis. *Cell Metab*. 2023;3(35):1752–66. e8.
- Brocker CN, Kim D, Melia T, Karri K, Velenosi TJ, Takahashi S, Aibara D, Bonzo JA, Levi M, et al. Long non-coding RNA Gm15441 attenuates hepatic inflammasome activation in response to PPARA agonism and fasting. *Nat Commun*. 2020;17(11):5847.

27. Brocker CN, Patel DP, Velenosi TJ, Kim D, Yan T, Yue J, Li G, Krausz KW, Gonzalez FJ. Extrahepatic PPAR α modulates fatty acid oxidation and attenuates fasting-induced hepatosteatosis in mice. *J Lipid Res.* 2018;59:2140–52.
28. Chyau CC, Wang HF, Zhang WJ, Chen CC, Huang SH, Chang CC, Peng RY. Antrodan alleviates high-fat and high-fructose diet-induced fatty liver disease in C57BL/6 mice model via AMPK/Sirt1/SREBP-1c/PPAR γ pathway. *Int J Mol Sci.* 2020;6:21.

Publisher's Note

Springer Nature remains neutral with regard to jurisdictional claims in published maps and institutional affiliations.